A Comparison of WSR-88D Storm Total Precipitation Performance during Two Tropical Systems following Changes to the Multiplicative Bias and Upper Reflectivity Threshold

Peggy Glitto

National Weather Service, Melbourne, Florida

Lt. Barry Choy

Airborne Snow Survey Program, National Operational Hydrologic Remote Sensing Center, Chanhassen, Minnesota

ABSTRACT

Seventy-two hours of Melbourne, Florida (KMLB), Weather Surveillance Radar 1988 Doppler (WSR-88D) rainfall data were compared with rain gauge data during Tropical Storm Gordon as it impacted east-central Florida. Comparisons were made by centering arrays of 9 and 25 storm total precipitation (STP) data bins over corresponding rain gauge locations, then performing bias and dispersion calculations prescribed by the Operational Support Facility (OSF). Findings indicate that the STP significantly underestimated rainfall during Tropical Storm Gordon and the magnitude of error varied with range from the radar. Based on these findings, it was recommended that the upper reflectivity threshold be increased to 55 dBZ and the multiplicative bias be set to 1.4 as an immediate but interim measure to minimize the differences between the STP and surface rain gauges during tropical systems. These recommended changes were given approval by the OSF and were deployed on the KMLB WSR-88D for a 72-h period as Tropical Storm Jerry affected east-central Florida. Significant improvement was noted in the STP product during Tropical Storm Jerry. Future studies will utilize base data replay capabilities to manipulate algorithms, biases, and thresholds individually and collectively to develop better radar rainfall adjustment schemes. Future work will also involve deploying tropical rainfall Z–R relationships that should further improve on the WSR-88D's rainfall estimation capability during tropical systems.

1. Introduction

The Weather Surveillance Radar 1988 Doppler (WSR-88D) rainfall algorithms have provided an automated and efficient method of producing radar rainfall estimates. Forecasters previously relied on estimates from satellite and radar performed over crude spatial and temporal scales. The WSR-88D precipitation products (1-h precipitation, OHP; 3-h precipitation, THP; and storm total precipitation, STP) have a spatial resolution of $1° \times 1.1$ nmi (2.04 km) and temporal resolution ranging from 5 min to several days. The automation, dramatically improved resolution, and increased coverage achieved with the WSR-88D rainfall algorithms have made these products beneficial for analyzing rainfall and recognizing flood potential.

The WSR-88D rainfall data is being used by National Weather Service (NWS) forecasters for flood statements and warnings and will be integrated to compute basin total rainfall and runoffs for river statements and warnings. For forecasters at the National Weather Service Office (NWSO) in Melbourne, Florida (KMLB), the performance of the WSR-88D rainfall algorithms during tropical systems has been of particular interest, due to the area's susceptibility to such systems.

The 1994 and 1995 Atlantic hurricane seasons provided meteorologists with an abundance of tropical cyclone data, with seven named tropical systems making landfall in Florida. Postanalyses of previous landfalling tropical systems in the Florida panhandle (Alberto in July 1994 and Beryl in August 1994) indicated that the NWSO Tallahassee WSR-88D precipitation products substantially underestimated rainfall. During Alberto, 60-h STP totals underestimated rainfall by 30% to more than 50% as compared to surface-based rain gauge reports (Mauro 1994). If not adjusted, further significant underestimation of tropical cyclone rainfall amounts could lead to delays in effective flash flood or river flood warnings.

In response to the ineffectiveness of the STP in tropical systems, the Operational Support Facility (OSF) developed a statistical scheme that allowed individual NWSOs to evaluate STP accumulations and compare

Corresponding author address: Ms. Peggy Glitto, National Weather Service, 421 Croton Road, Melbourne, FL 32935.
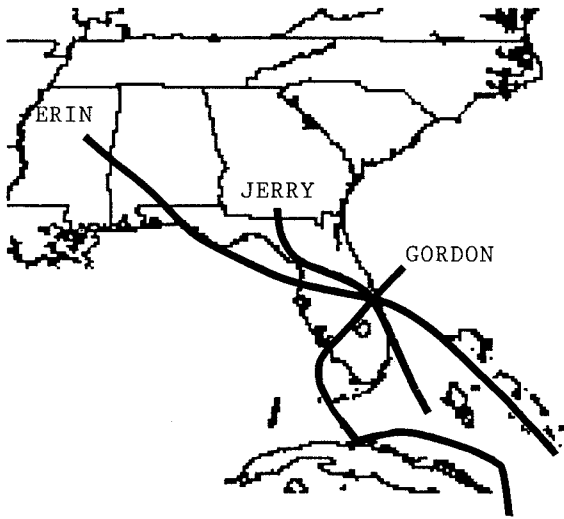E-mail: peggy.glitto@NOAA.gov

FIG. 1. Tracks of Tropical Cyclones Erin, Gordon, and Jerry as they moved across central Florida.

those with surface-based rain gauge accumulations. This statistical scheme was based largely on the work of Wilson and Brandes (1979), in which mean radar rainfall estimates were adjusted by matching the radar rainfall estimates with correspondent gauge readings. After the OSF scheme was distributed in late 1994, three other storms (Erin, Gordon, and Jerry; Fig. 1) would give NWSO Melbourne an opportunity to evaluate the statistical scheme and suggest improvements. Heavy rains and subsequent flooding were a major problem across parts of the central peninsula as Gordon, Erin, and Jerry moved over the area. In November 1994, Tropical Storm Gordon developed and moved over the central Florida area, well within the range of the KMLB WSR-88D. A 72-h study of STP performance was conducted during Gordon (14–17 November 1994), and based on the results, a short-term approach to correcting rainfall estimates was recommended. Procedures were developed that allowed for simple on-site adaptable parameter adjustments that would improve WSR-88D rainfall estimation.

The recommended parameter adjustments were employed on the KMLB WSR-88D prior to Tropical Storm Jerry's influence on central Florida, 23–26 August 1995. The rainfall accumulation data collected as Jerry moved over central Florida provided the opportunity for a comparison of rainfall estimation with gauge verification for two tropical systems of comparable strength and duration over the same area, before and after simple corrective measures were implemented. These measures are detailed in the following sections. Section 2 describes the WSR-88D rainfall algorithms and the rain gauge network used in the study. Section 3 describes methods used to compare the STP data with rain gauge data. Section 4 presents the analysis results from the Gordon study, the proposed changes to the rainfall algorithm thresholds based on the study, and analysis of the subsequent STP performance after the proposed changes were implemented during the Jerry event. Finally, the discussion will summarize the benefits of changing the rainfall algorithm thresholds and outline the proposed changes to further improve STP performance.

2. Background

a. Rainfall algorithms

Rainfall estimated over a 124 nmi (230 km) radius of coverage by the WSR-88D is accomplished using a system of algorithms. The precipitation processing subsystem uses a hybrid scan construction to provide continuity between the base reflectivity sample volumes that are used to compute rainfall rates. A detailed description of hybrid scan construction and precipitation processing algorithms is available in *Federal Meteorological Handbook* 11—Part C (OFCM 1991). The hybrid scan uses reflectivity values from four low-level elevation slices, dependent on range from the radar data acquisition unit (RDA, Fig. 2), with elevation angles increasing closer to the RDA. This is done to ensure that all sample volumes are taken from approximately 3000 ft (1 km). At ranges beyond 27 nmi (50 km) from the radar, biscan maximization chooses the maximum sample volume between the $0.5°$ and $1.5°$ elevation slices
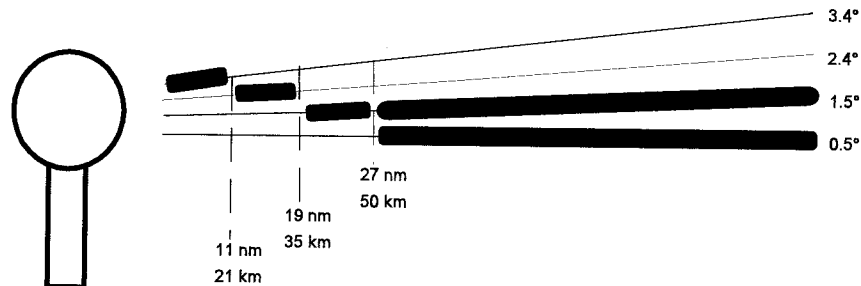

FIG. 2. The WSR-88D hybrid scan construction. The WSR-88D uses higher elevation angles close to the radar and lower angles as distance from the radar increases to maintain nearly uniform sampling height above the surface (under standard refractive conditions). This graphical depiction illustrates the elevation angles used at the various distances from the RDA.

to minimize errors due to contamination by ground clutter.

Rainfall rates (R) are computed for each sample volume by inputting the base reflectivity (Z) from the sectorized hybrid scan and using the equation $Z = 300R^{1.4}$. The sample volume sizes are adjusted for uniformity, since the beam volume increases with range, then corrections are applied for time continuity and beam filling at distant ranges. The corrected rainfall rates for each sample volume are then converted to rainfall accumulations, which are output to the user as the following graphical displays (Klazura and Imy 1993): OHP (total from the past hour, updated each volume scan), THP (total from the past three clock hours, updated on the hour), and STP (total accumulated precipitation since the first volume scan with detected precipitation or since the STP was last reset, updated each volume scan).

There are many potential sources of error despite the complex system of quality checks in the radar system. Errors in rainfall rate and rainfall accumulation may stem from below-beam effects that may skew rainfall estimation by missing intense low-level precipitation, precipitation phase (rain versus hail or snow), and vertical distribution of precipitation. Errors may also arise due to gaps between volume scans and missing volume scans. The rainfall algorithms compensate for missing data by averaging data from the previous and following volume scans. Problems with hardware calibration, anomalous propagation, and wet radome attenuation may also result in errors. Site-adaptable thresholds are set to minimize the effect of spurious weak reflectivity returns and overestimation of rainfall due to hail contamination. Rainfall is not computed from reflectivity values below the lower default threshold of 18 dBZ, and all values above the upper default threshold of 53 dBZ are truncated to 53 dBZ. Using the 53-dBZ threshold and the current Z–R relation, it is not possible to realize rainfall rates in excess of 4.09 in. (103.8 mm) h^{-1}. This may be a source of error in tropical environments where rainfall rates in excess of this limit are often observed in the absence of any hail reaching the surface. Additionally, the Z–R relationship may not be representative of the average drop size distribution. Errors in rainfall rate and accumulation may also exist due to below-beam effects that may skew rainfall estimation by missing intense low-level precipitation, evaporation of rain drops below the sampling altitude, or redistribution of precipitation by strong horizontal wind.

In the future, using a network of rain gauges, rainfall rates will have a bias computed and a correction applied hourly during the event. Once implemented, a Kalman filter (Ahnert et al. 1983) will compute a multiplicative bias between the radar precipitation estimates from the best of nine bins (centered over the gauge) and real-time rain gauge measurements from the gauge data acquisition system on an hourly basis. This is designed to correct for systematic radar biases.

TABLE 1. Percentage of gauge types used in the Gordon and Jerry studies.

Gauge type	Gordon (%)	Jerry (%)
GOES	25	26
NWS/cooperative	39	13
ALERT/SCADA	36	49
NASA	—	12

b. Rain gauge network

The central Florida area has a dense rain gauge network. The St. Johns River Water Management District operates and maintains a telemetry tipping bucket rain gauge network (known as ALERT) over much of east-central Florida. The network is connected to a main data collection and storage facility in Palatka, Florida, from where it may be accessed remotely via computer and modem. In support of the WSR-88D evaluation as part of National Aeronautics and Space Administration (NASA) Tropical Rainfall Measuring Mission, the NWSO MLB was provided with access to ALERT gauge data directly or through the main computer. An archived database of rain gauge data may be queried at various time increments. This data, along with cooperative observing sites and NWS sites, produced over 200 surface point rainfall data sources within the 124 nmi (230 km) radius of radar coverage. Of the available gauges, 122 reported useful time-matched readings for the 72 h of data used in the Gordon study. Additionally, during Gordon, one of the 122 gauges was an optical rain gauge located on a weather data buoy about 20 nmi (37 km) off the coast of Cape Canaveral.

Southwest Florida Water Management District Supervisory Control and Data Acquisition (SCADA) gauge data were used during Jerry, when heavy rain was widespread over the SCADA gauge coverage area. The SCADA gauges are accessed via computer and modem in a similar fashion to the ALERT gauges. NWS/cooperative observer site gauges were also used during both events, which included several South Florida Water Management District sites. Additionally, totals from 18 tipping bucket gauges maintained by NASA and located near the Kennedy Space Center were used during Jerry. For the 72 h of data used in the Jerry study, 154 gauges reported useful time-matched readings. Table 1 lists the percentage of gauge types used during Gordon and Jerry. Figures 3a and 3b show locations of gauges used during Gordon and Jerry, and isohyets of rainfall totals recorded by the gauges. Within the 124 nmi (230 km) radius of radar coverage, maximum 72-h gauge-accumulated rainfall totals were nearly 16 in. (406 mm) during Gordon and above 18 in. (457 mm) during Jerry. However, the majority of the gauges recorded below 10 in. (254 mm) during both cases (Figs. 4a and 4b).

Since the majority of rain gauges used in the comparison were tipping bucket gauges, it was noted that the gauges could have underestimated rainfall during

a

FIG. 4. Frequency distribution of measured rainfall totals for (a) Gordon and (b) Jerry.
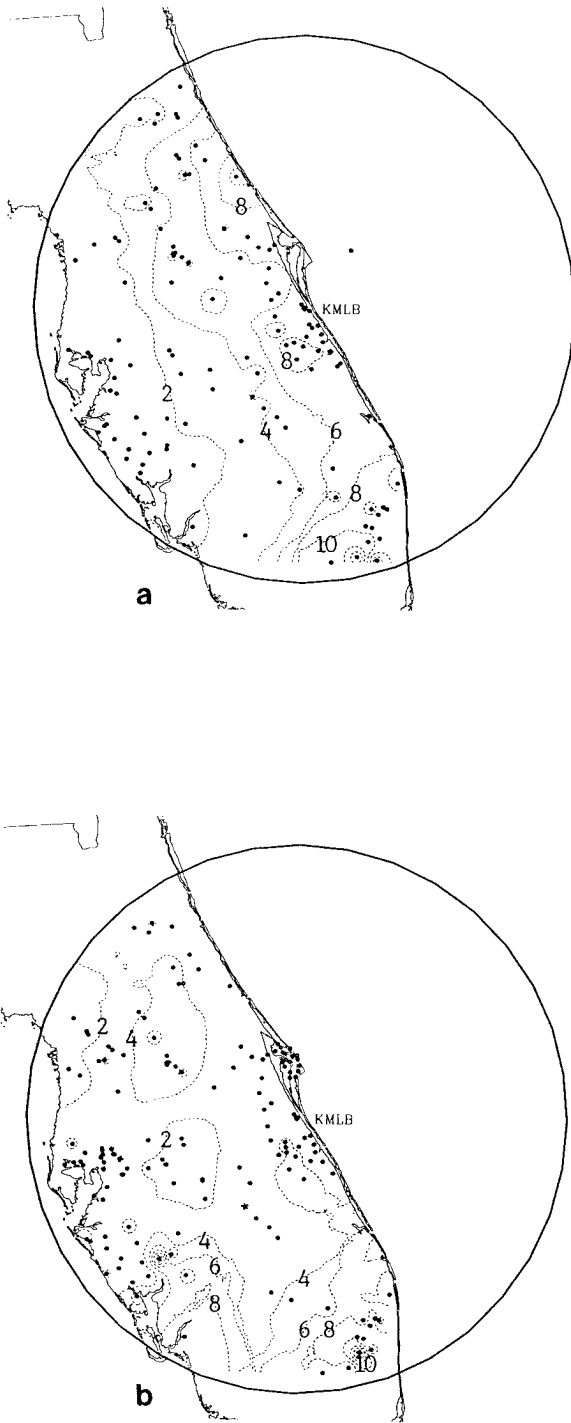

b

FIG. 3. Location of gauges used during the (a) Gordon and (b) Jerry cases, and isohyets of rainfall amounts recorded by gauges [isohyets at every 2 in. (5.08 cm)].

the Gordon and Jerry events. According to Linsley et al. (1982), tipping bucket gauges may underestimate by 5% at rain rates of 5–6 in. (125–150 mm) h^{-1}. Furthermore, with rainfall underestimation of 5% expected at wind speeds of 20 mph (8.9 m s^{-1}), a more serious
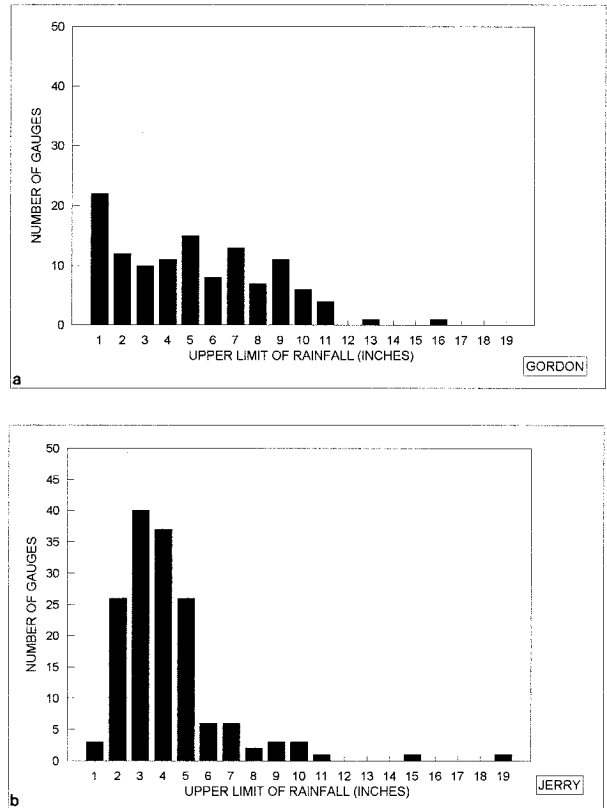
deficiency of the measurement is expected due to wind, since tropical storm force winds far exceed this value. Consequently, as a result of heavy rainfall rates and strong winds, tipping bucket gauges may have underestimated total rainfall realized at the surface by at least 10% during tropical storms, compounding the radar–ground verification differences.

3. Methods

a. Archiving STP data

Each precipitation product is stored in a background file at the radar products generator (RPG). For the STP product, the file HYPROD.DAT contains a running total of estimated rainfall between resets of the STP. A reset of the STP sets all rainfall accumulation files to zero. The STP was reset close to 1200 UTC prior to the Gordon and Jerry events to coincide with rain gauge reset time, as 24-h rainfall is commonly reported ending at 1200 UTC. After each heavy rain event, the HYPROD.DAT file was copied onto the Small Computer Systems Interface tape at the RPG, also close to 1200 UTC. The HYPROD.DAT files stored 72 h of data for both the Gordon and Jerry events. These data were used to perform a comprehensive statistical comparison be-
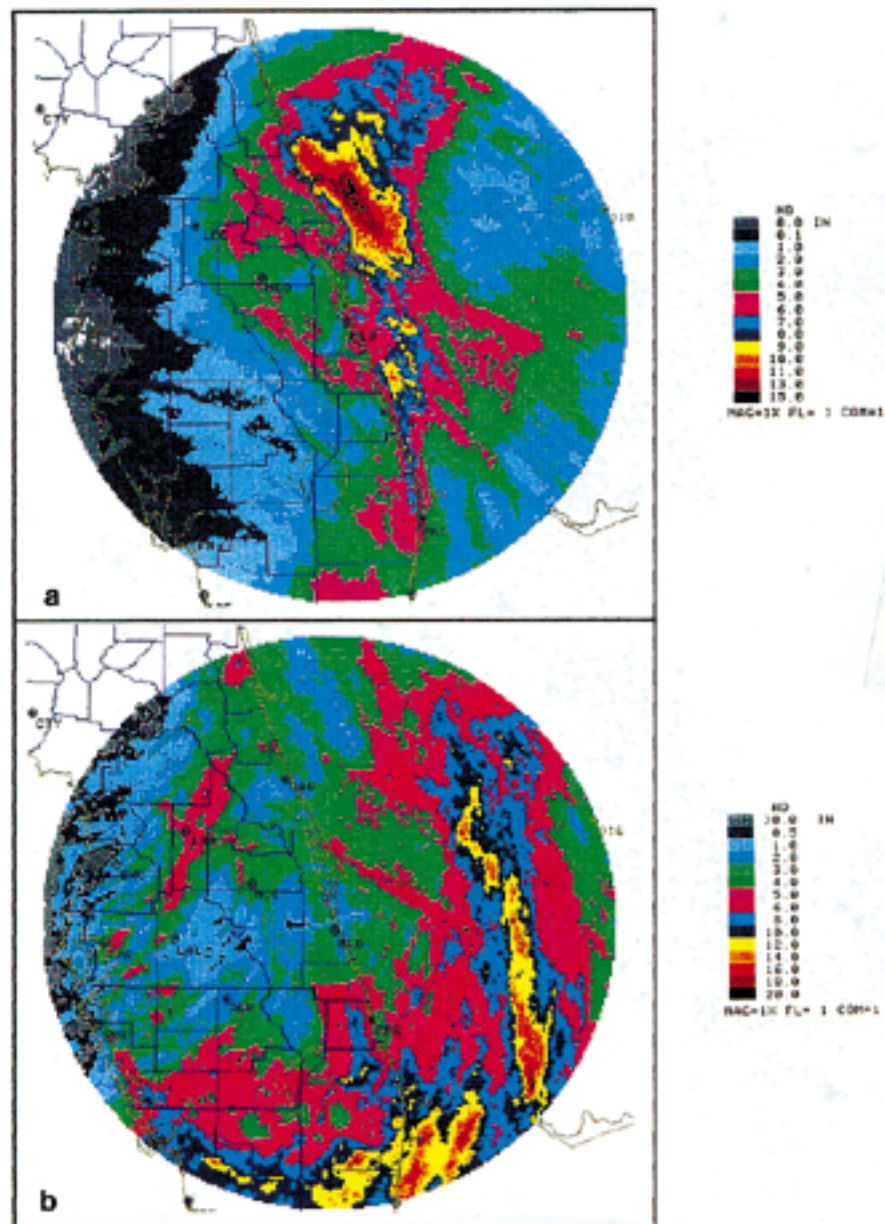
FIG. 5. The 72-h STP for (a) Gordon and (b) Jerry. The reader should note that while the data table colors are the same for both cases, the values are different.

tween radar estimated rainfall (Figs. 5a and 5b) and rain gauge totals.

b. Gauge to radar comparison

The archived HYPROD.DAT files were forwarded to the OSF where STP rainfall amounts to the nearest 0.01 in. (0.254 mm) were overlaid on the available gauges within 124 nmi (230 km) of the KMLB WSR-88D (Fig. 6). Even with gauge latitude–longitude positions available as close as the nearest second, it is unlikely that the actual gauge position was always centered directly under the center bin. Therefore, the accumulations were compared to an array of STP bins that were approximately centered over a particular gauge. The center, best fit, maximum, minimum, and average of nine bins were each compared with the corresponding gauge to evaluate the WSR-88D representation of total rainfall that occurred during the 72 h of rainfall from the tropical system. Additionally, a 25-bin analysis was performed using the best fit, maximum, and minimum bins. The results were then compared to the 72-h surface gauge accumulations.

Once the rain gauge data is incorporated into the rain-

```
0101:      AZ=181.6 Range=52.7 km
Km \ Az 179.5 180.5 181.5 182.5 183.5
```

57	4.71	4.73	4.79	4.88	4.68
55	4.76	4.83	5.19	4.66	4.73
53	5.53	5.22	5.38*	5.26	5.67
51	5.52	5.73	5.38	5.37	5.54
49	5.04	4.94	4.35	4.55	4.48

```
        MAX: 5.73  MIN: 4.66  AVG: 5.22
```

*Center bin is centered over gauge location.
MAX, MIN, and AVG are for 9 bins (closest to gauge location).

FIG. 6. The 5 × 5 matrix of output received from OSF for 25 STP bins centered over gauge 0101 with MAX, MIN, and AVG listed for the 9 center bins. The azimuth (top) and range (left) of each bin define its location with respect to the RDA (KMLB WSR-88D).

fall algorithms, the algorithms will use what is considered the best match of nine bins surrounding the gauge location (referred to as best bin hereafter). If the gauge value is between the maximum and minimum thresholds, it will use the gauge value as the best bin. If the gauge is lower (higher) than the minimum (maximum) of the nine bins, the minimum (maximum) is used as the best bin. Calculations using the center bin and best bin (which should best approximate gauge-estimated rainfall) will be presented in this study.

c. Calculations

A statistical analysis was performed to determine how well the radar performed under the current system as compared to how well it may be expected to perform with corrections. These analyses were developed to simulate the WSR-88D's processing of radar–gauge data and to standardize the output the OSF received from participating offices. Mean radar bias [(Eq. (1) and Eq. (2)], relative dispersion [variance—Eq. (3)], and average difference [AD—Eq. (4) and Eq. (5)] were calculated as prescribed by the OSF (Klazura and Kelly 1995):

$$\text{Mean radar bias} = \frac{\sum_{i=1}^{N} G_i}{\sum_{i=1}^{N} R_i} \qquad (1)$$

$$\text{Mean radar bias} = \frac{1}{N} \sum_{i=1}^{N} \frac{G_i}{R_i} \qquad (2)$$

(G = gauge and R = radar in each of the equations).

The main difference between Eqs. (1) and (2) is that in Eq. (1) the radar values are weighted proportionate to the gauge amount and in Eq. (2) each gauge to radar comparison has an equal weight. The subsequent calculations used Eq. (2) since the focus was on heavy rain

and Eq. (1) may be influenced by large gauge readings typical with tropical systems. For both Eq. (1) and (2), values higher (lower) than 1 indicate underestimation (overestimation) by the radar.

Equation (3) describes the amount that the radar values were scattered from the gauge value, with larger dispersions resulting from larger standard deviation values:

$$\text{Variance} = \frac{\sigma[G/R]}{G/R} 100\%. \qquad (3)$$

Equation (4) is the percentage by which the radar varied from the gauge (both higher and lower):

$$\text{AD} = \frac{1}{N} \sum_{i=1}^{N} \left| \frac{(G_i - R_i)}{G_i} \right| 100\%. \qquad (4)$$

Equation (5) represents the average difference with the mean radar bias computed in Eq. (2) applied as a correction:

$$\text{AD} = \frac{1}{N} \sum_{i=1}^{N} \left| \frac{[G_i - (\overline{G/R})R_i]}{G_i} \right| 100\%. \qquad (5)$$

Equations (2)–(5), the values were recalculated after removing values that were not within two standard deviations of the mean radar bias.

Calculations for the Jerry study were performed using the same set of equations as for the Gordon study, but with the approved changes made to the rainfall algorithm thresholds (discussed in section 4b) before the onset of Jerry's rainfall across the radar coverage area. Calculations from the Gordon study and subsequent algorithm threshold changes will be discussed in the next section.

4. Results

a. Results from Gordon study

The Gordon rainfall study (Choy et al. 1996) showed that the KMLB WSR-88D STP product underestimated rainfall (as compared to gauges) by approximately 40% over the entire radar range (Table 2). The Gordon study further indicated that the distribution of differences between STP and gauge was not uniform, but greater differences existed within 27 nmi (50 km) and beyond 90 nmi (167 km). Within 27 nmi (50 km) the mean radar bias indicated severe underestimation by the radar with values ranging from 1.47 to 2.35 for the center and best bins (Table 3). Beyond 90 nmi (167 km) severe underestimation was again noted, with values for the center and best bin ranging from 2.33 to 4.01 (Table 4). In the 27.1–90 nmi (50–167 km) range, underestimation was not as severe as the other ranges, with bias values for the center and best bin ranging from 1.57 to 1.28 (Table 5). More details on the Gordon results will be presented in section 4c, when results from Gordon are compared with results from Jerry.

TABLE 2. Output from center bin and best bin for Gordon and Jerry over entire radar range.

Equation	Gordon		Jerry	
	Center	Best	Center	Best
Mean radar bias [Eq. (1)]	1.65	1.44	0.83	0.91
Mean radar bias [Eq. (2)]	2.58	1.88	0.92	0.95
Adj radar bias [Eq. (2*)]	2.05	1.57	0.87	0.92
Relative dispersion [Eq. (3)]	128%	117%	46%	32%
Adj relative dispersion [Eq. (3*)]	71%	41%	37%	19%
Average diff [Eq. (4)]	48%	37%	38%	18%
Adj average diff [Eq. (4*)]	46%	35%	36%	17%
Average diff 2 [Eq. (5)]	76%	46%	32%	18%
Adj average diff 2 [Eq. (5*)]	49%	30%	28%	17%

* Recalculated after removing G/R values not within two standard deviations of the mean.
Adj = adjusted.
Diff = difference.

TABLE 4. Output from center bin and best bin for Gordon and Jerry for 90.1–124 n mi (167–230 km) range.

Equation	Gordon		Jerry	
	Center	Best	Center	Best
Mean radar bias [Eq. (1)]	1.93	1.77	0.72	0.83
Mean radar bias [Eq. (2)]	4.01	2.80	0.84	0.90
Adj radar bias [Eq. (2*)]	2.79	2.33	0.78	0.87
Relative dispersion [Eq. (3)]	125%	124%	47%	28%
Adj relative dispersion [Eq. (3*)]	80%	69%	40%	24%
Average diff [Eq. (4)]	57%	47%	55%	27%
Adj average diff [Eq. (4*)]	54%	44%	55%	26%
Average diff 2 [Eq. (5)]	104%	65%	39%	24%
Adj average diff 2 [Eq. (5*)]	53%	49%	36%	23%

* Recalculated after removing G/R values not within two standard deviations of the mean.
Adj = adjusted.
Diff = difference.

b. Proposed changes from Gordon study

Following the Gordon study, we proposed that a short-term solution to improving the STP estimations during tropical systems would be to change the maximum rainfall (MXRFL) threshold from 53 to 55 dBZ during the traditional Florida "wet" season (30 May–30 September). This would allow maximum rainfall rates to increase from 4.09 in. (103.8 mm) h^{-1} to 5.68 in. (144.2 mm) h^{-1}. This proposed change was based on the increased depth of the melting layer during the wet season and previously observed rainfall rates in Florida that exceeded the 4.09 in. (103.8 mm) h^{-1} rates allowed by the 53-dBZ maximum reflectivity threshold (Fernald and Patton 1984). The Gordon study also proposed a change of the multiplicative bias (RESBI) from 1.0 to 1.4, which would effectively increase all STP values by 40% when a tropical system is expected to affect the KMLB radar coverage area. These proposals were approved by the OSF algorithm section on a trial basis. Based on this authorization, the KMLB WSR-88D MXRFL and RESBI thresholds were changed to

the newly approved tropical thresholds upon the onset of Tropical Storm Jerry's impact over the radar coverage area in August 1995.

c. Comparison of results from Jerry and Gordon studies

1) CENTER BIN

Center bin calculations were performed in order to compare the radar to gauges with no corrections (Figs. 7a and 7b). Over the entire range (Table 2), the mean radar bias in Eqs. (1) and (2) both indicated that the radar severely underestimated rainfall measured by the gauges during Gordon, with center bin values of 1.65 and 2.58, respectively. During Jerry, these biases were much lower with only a slight overestimation indicated [Eqs. (1) and (2) for center bin were 0.83 and 0.92]. Since tipping bucket gauges often underestimate rainfall amounts during heavy rain and high winds, the underestimation during Gordon may have actually been worse than these values indicated, although the amount is unknown. Similarly, the overestimation during Jerry may actually be less than the values

TABLE 3. Output from center bin and best bin for Gordon and Jerry for 0–27 n mi (0–50 km) range.

Equation	Gordon		Jerry	
	Center	Best	Center	Best
Mean radar bias [Eq. (1)]	1.79	1.47	1.00	1.02
Mean radar bias [Eq. (2)]	2.35	1.53	1.05	1.05
Adj radar bias [Eq. (2*)]	2.04	1.43	0.99	0.98
Relative dispersion [Eq. (3)]	81%	35%	39%	36%
Adj relative dispersion [Eq. (3*)]	65%	23%	20%	11%
Average diff [Eq. (4)]	44%	32%	34%	9%
Adj average diff [Eq. (4*)]	42%	30%	18%	7%
Average diff 2 [Eq. (5)]	63%	22%	21%	13%
Adj average diff 2 [Eq. (5*)]	46%	17%	17%	8%

* Recalculated after removing G/R values not within two standard deviations of the mean.
Adj = adjusted.
Diff = difference.

TABLE 5. Output from center bin and best bin for Gordon and Jerry for 27.1–90 n mi (50–167 km) range.

Equation	Gordon		Jerry	
	Center	Best	Center	Best
Mean radar bias [Eq. (1)]	1.45	1.28	0.89	0.96
Mean radar bias [Eq. (2)]	1.57	1.33	0.91	0.95
Adj radar bias [Eq. (2*)]	1.53	1.32	0.91	0.92
Relative dispersion [Eq. (3)]	29%	25%	46%	29%
Adj relative dispersion [Eq. (3*)]	24%	20%	46%	17%
Average diff [Eq. (4)]	44%	31%	33%	16%
Adj average diff [Eq. (4*)]	34%	23%	33%	15%
Average diff 2 [Eq. (5)]	34%	27%	26%	15%
Adj average diff 2 [Eq. (5*)]	16%	15%	26%	15%

* Recalculated after removing G/R values not within two standard deviations of the mean.
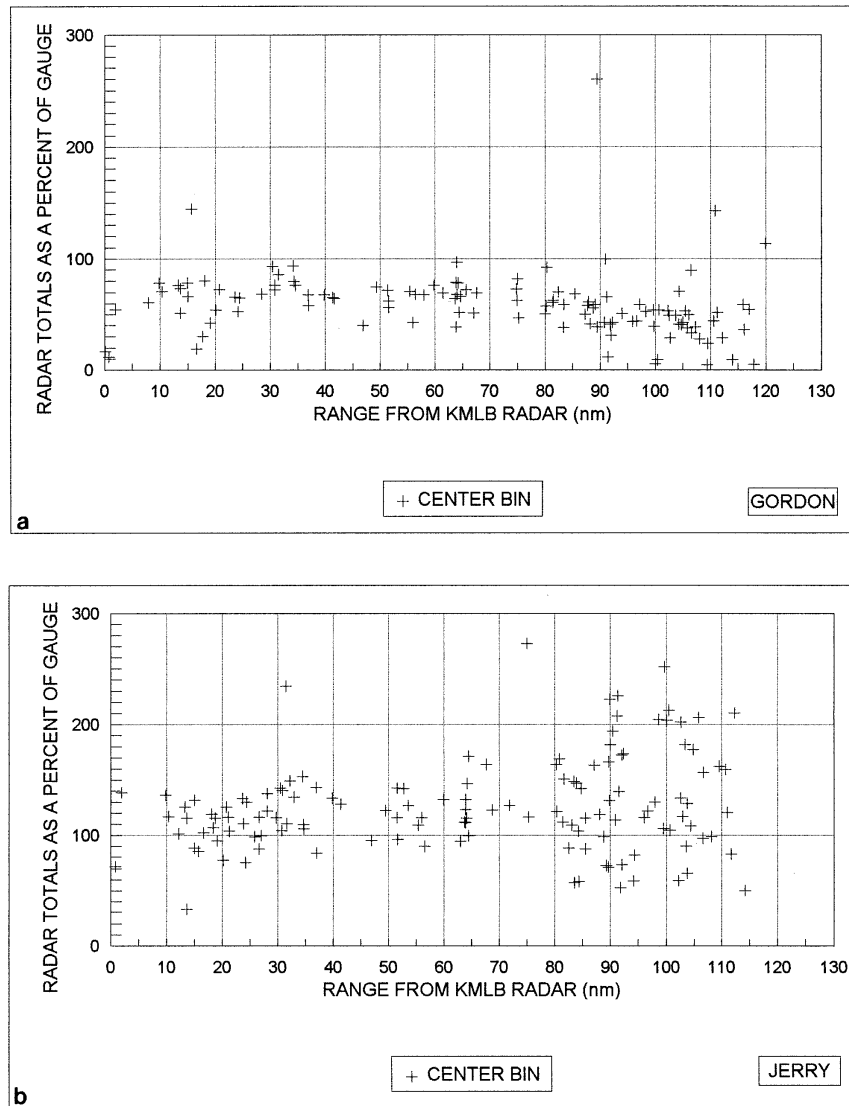Adj = adjusted.
Diff = difference.

FIG. 7. Center bin radar-estimated values plotted as a percent of the gauge totals for (a)
Gordon and (b) Jerry.

show. Within 27 nmi (50 km) [number of gauges (n) = 21 for Gordon, $n = 30$ for Jerry], the mean radar bias was very close to 1 for Jerry, while significant underestimations were indicated during Gordon. At the 27.1–90 nmi (50–167 km) range ($n = 57$ for Gordon and $n = 72$ for Jerry) the mean radar bias during Gordon again indicated a large underestimation by the radar, while during Jerry the values on average indicated only a small overestimation. At the 90.1–124 nmi (167–230 km) range ($n = 44$ for Gordon and $n = 52$ for Jerry), the mean radar bias during Gordon indicated severe underestimation by the radar, and a relatively small overestimation during Jerry (again considering that tipping bucket gauges may underestimate rainfall). The relative dispersion (variance) [RD—Eq. (3)] was much lower during Jerry for the center bin over the entire range, and at each range segment ex-

amined, except for the 27.1–90 nmi (50–167 km) range. Figure 8a shows the AD before a bias correction was applied [Eq. (4)], and Fig. 8b shows the AD after the bias correction was applied and values not within 2 standard deviations were removed [Eq. (5*)]. For the center bin, the uncorrected AD decreased during Jerry for each range segment examined. After the correction was applied, the AD decreased more significantly at each range during Jerry, except at the 27.1–90 nmi (50–167 km) range, where it increased. The need to make bias adjustments range-specific in the future is apparent here.

2) BEST BIN

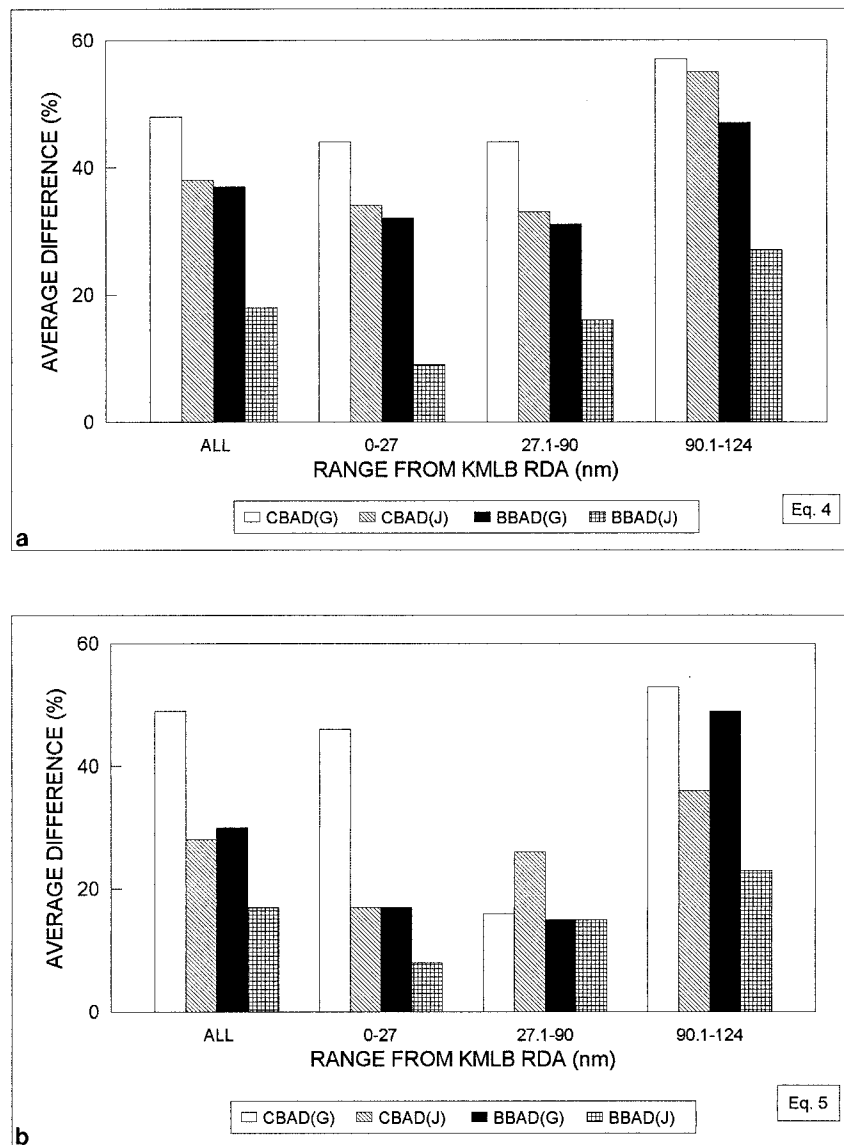Computing the same parameters for the best match of the nine bins over the entire range (Table 2), the

FIG. 8. Average differences before applying a bias correction (a) and after applying a bias correction (b): CBAD(G) = center bin during Gordon, CBAD(J) = center bin during Jerry, BBAD(G) = best bin during Gordon, and BBAD(J) = best bin during Jerry.

mean radar bias in Eqs. (1) and (2) indicated that the radar severely underestimated rainfall measured by the gauges during Gordon, with best bin values 1.44 and 2.58, respectively. During Jerry, these biases were much lower with only a slight overestimation indicated (bias for best bin 0.91 and 0.95). Within 27 nmi of the radar, the mean radar bias during Jerry was very close to 1, while large rainfall underestimations were indicated by the radar during Gordon (Figs. 9a and 9b). At the 27.1–90 nmi (50–167 km) range, the mean radar bias was much closer to 1 during Jerry than during Gordon. At 90.1–124 nmi (167–230 km), mean radar bias indicated significant underestimation by the radar during Gordon and only slight overestimation during Jerry. The relative

dispersions during Jerry were much smaller than during the Gordon case. The AD improved for the 0–27 nmi (0–50 km) and the 90.1–124 nmi (167–230 km) ranges but showed no improvement in the 27–90 nm (50–167 km) range.

d. Results of Jerry without 1.4 multiplicative bias

To determine the importance of increasing the multiplicative bias to 1.4 during Jerry, the Jerry case was recomputed with RESBI = 1.0 and MXRFL = 55 dBZ, for the center and best bin (Figs. 10a and 10b). The best bin was recalculated after the max and min bins were divided by 1.4, to show if the gauge values were within
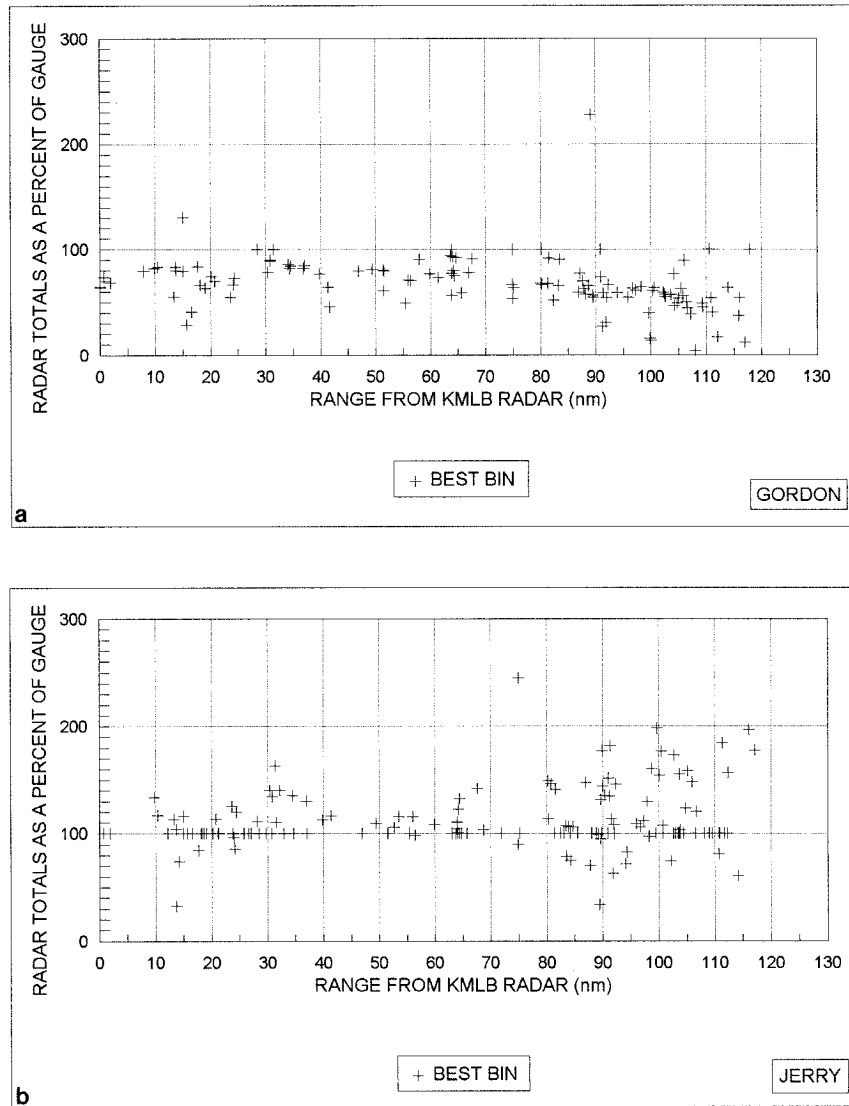
FIG. 9. The best of nine bin radar-estimated values plotted as a percent of the gauge totals for (a) Gordon and (b) Jerry.

the lower and upper thresholds. There are noticeably more values along the 100% line for the best bin than for the center bin. This is a function of the number of times the gauge value was between the max and min bin values; the larger the difference between the max and min bins, the greater the probability of the gauge falling between the values.

Since the center bin is not influenced by the gauge reading as the best bin is, the center bin values were examined for RESBI of 1.4, 1.2, and 1.0. The mean radar bias [Eq. (2)] over the entire range at a 1.4 RESBI was 0.92. For a 1.2 RESBI, the mean radar bias was 1.07, and for a 1.0 RESBI it was 1.28. These values indicate that with the default RESBI of 1.0 the radar would have underestimated rainfall by nearly 30% over the entire range. Slight overestimation occurs with 1.4

RESBI and slight underestimation occurs with a 1.2 RESBI; an optimal RESBI for this case would be somewhere between 1.2 and 1.4. The RESBI increase to 1.4 had more influence on the results than the 55-dBZ threshold increase by itself, as the default RESBI still would result in nearly 30% underestimation by the radar for this case.

5. Discussion and conclusions

a. Changing threshold reflectivity and multiplicative bias

By increasing the maximum upper threshold reflectivity from 53 to 55 dBZ and increasing multiplicative bias by 40% to 1.4, a significant improvement was noted
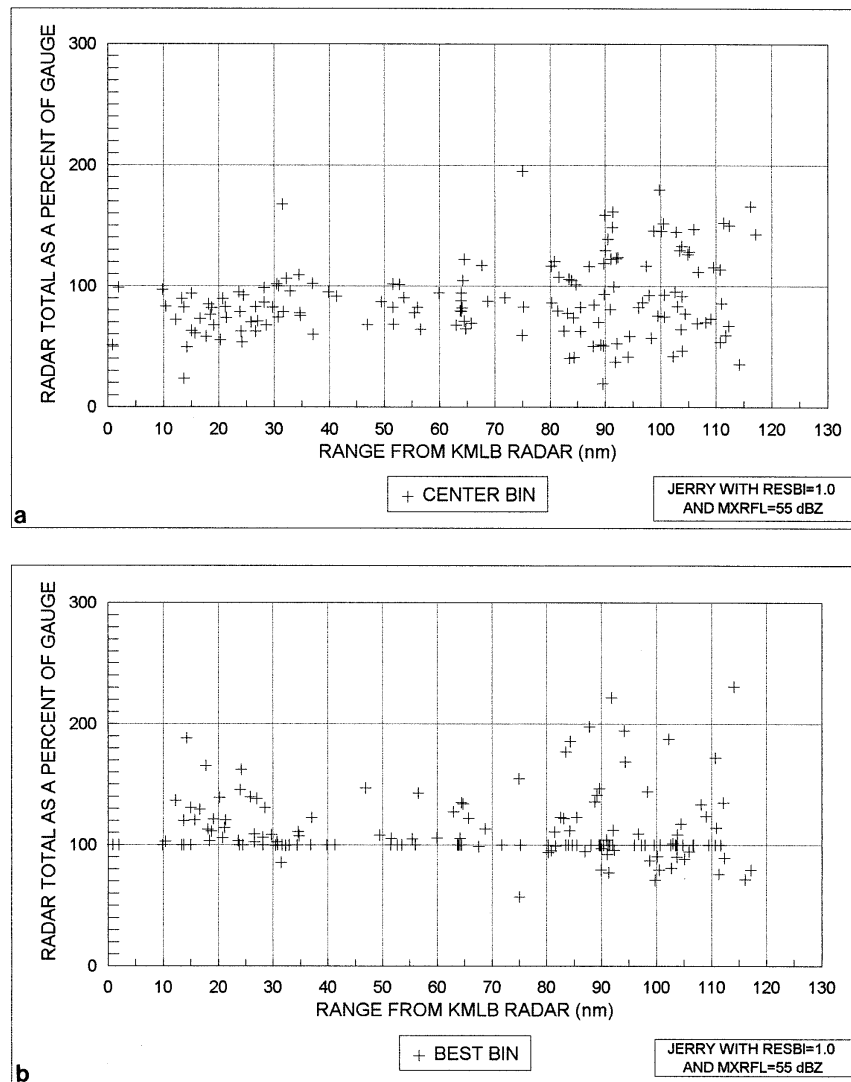
FIG. 10. Center bin and best bin radar-estimated values plotted as a percent of actual measured rainfall for all gauges during Jerry, with the MXRFL set at 55 dBZ but the RESBI decreased to 1.0.

in STP rainfall estimation during Tropical Storm Jerry, especially within 27 nmi (50 km) and beyond 90 nmi (167 km) from the radar. Beyond 27 nmi (50 km), below-beam effects most likely contributed to a large portion of the difference between the radar-estimated and gauge-measured totals. The heavier rainfall estimates realized with the changed thresholds gave forecasters a better indication of the flood threat in real time. This allowed for a proactive approach to issuing flood products during the events. Additional knowledge gained through future work will provide better lead times on flood warnings and statements.

It is important to note that the postanalysis results would not necessarily reflect real-time correction results. In the cases of Gordon and Jerry, well over 100 gauges were used, and many of these did not have hourly

resolution. In real time, only 50 gauges will be available, and since many of the gauges may not have rainfall during a given event, only a fraction of the 50 gauges may be available in real time. In the future, the network of gauges is planned to increase to 200 (Fulton et al. 1995), which will improve the ground validation. Additionally, in real time, multiplicative bias and other corrections would be applied on an hourly basis and therefore will be changing more frequently than in this study.

b. Changing Z–R relationships and other proposals to improve rainfall estimations

In order to correctly adjust radar-estimated rainfall, it is necessary to understand the major error components
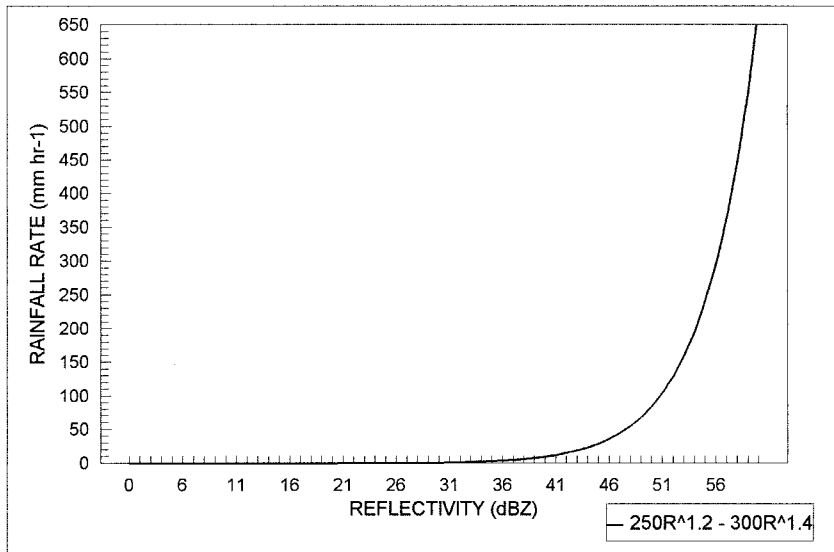
Fɪɢ. 11. Rainfall rates produced by the default *Z–R* relationship subtracted from the tropical *Z–R* relationship, for various dBZ levels.

and that each may not contribute equally during all weather situations. For example, the default *Z–R* relationship may work for the most intense cells within a tropical system, but these cells may only represent a small fraction of the total rainfall. Low-topped cells producing heavy precipitation may be a large contributor, and the precipitation from these cells may be severely underestimated due to below-beam effects. The problem is compounded when the percent distribution of different types of rainfall changes as systems evolve.

A new *Z–R* relationship has been approved by the OSF for NWS offices to deploy during tropical rainfall, based on Rosenfeld et al. (1993), who stratified rainfall into four regimes and found that the *Z–R* relationship for a convective maritime regime roughly follows the power law of the form $Z = 250R^{1.2}$. At low reflectivity values, the differences in the rainfall rates between the new and default *Z–R* thresholds are negligible but increase rapidly for higher reflectivity values. Figure 11 shows that default *Z–R* relationship subtracted from the tropical *Z–R* relationship, which illustrates the rapidly increasing difference in rainfall rate for higher reflectivity values. The tropical *Z–R* relationship will be deployed for the KMLB radar whenever a tropical cyclone is expected to move into the radar coverage area.

While the proposed tropical *Z–R* relationship may help improve the STP estimations, other adjustments will be necessary to realize an optimal STP estimation. With respect to the radar, Seo and Johnson (1995) noted that problems with hybrid scan construction would be minimized with the following planned improvements: optimal construction of the hybrid scan, improvements to the precipitation adjustment algorithm, optimization of the adaptable parameters, anomalous propagation detection and removal, and corrections for bright band

noted in areas of mixed ice and liquid precipitation. Thus, a single multiplicative bias cannot reasonably correct for errors realized from several factors affecting the estimations to varying azimuth and range combinations and different precipitation types.

Meteorologically, we should strive to improve knowledge of the physical aspects of rainfall, especially drop size distributions. Temperature, moisture, instability, etc. should be evaluated to identify similarities and differences in types of events. Rainfall comparisons between similar events should be compared and event-specific parameters identified. For Florida, these events would include tropical moisture feeding along a stalled frontal boundary, the influence of a nearby tropical upper-tropospheric trough, and heavy rain associated with a tropical wave. Additionally, differences between overlapping WSR-88Ds should be identified through coordinated rainfall comparisons with nearby radars [for Melbourne, radars in Tampa (KTBW), Jacksonville (KJAX) and Miami (KAMX) could be used]. Capability to play back base radar data allows different thresholds and *Z–R* relationships to be tested and the best combination to be used.

Once the best combination of parameters are identified for different types of systems, then software can be developed to input model and environmental data into the radar and process this data to determine which areas of precipitation are convective, stratiform, and tropical/nontropical. The radar could then be tasked to apply the appropriate corrective measures and range-dependent thresholds and adjust estimated rainfall accordingly.

REFERENCES

Ahnert, P. R., M. D. Hudlow, E. R. Johnson, and D. R. Greene, 1983: Proposed ''on-site'' precipitation processing system for NEXRAD. Preprints, *21st Conf. on Radar Meteorology,* Edmonton, AB, Canada, Amer. Meteor. Soc., 378–385.

Choy, B. K., L. M. Mazarowski, and P. A. Glitto, 1996: Tropical Storm Gordon, 1996: 72-hr rainfall totals over east central Florida and WSR-88D comparisons. NOAA Tech. Memo. NWS-SR 174, 14 pp. [NTIS PB 96-163522.]

Fernald, E. A., and D. J. Patton, Eds., 1984: *Water Resources Atlas of Florida.* The Florida State University Foundation, 281 pp.

Fulton, R. A., D. J. Seo, J. P. Breidenbach, and E. R. Johnson, 1995: Performance of the WSR-88D radar-raingauge rainfall bias adjustment algorithm. *Proc. Third Int. Symp. on Hydrological Applications of Weather Radars,* Sao Paulo, Brazil, ABRH/IAHR, 109–117.

Klazura, G. E., and D. A. Imy, 1993: A description of the initial set of analysis products available from the NEXRAD WSR-88D system. *Bull. Amer. Meteor. Soc.,* **74,** 1293–1311.

——, and D. S. Kelly, 1995: A comparison of high resolution rainfall accumulation estimates from the WSR-88D precipitation algorithm with rain gage data. Preprints, *27th Conf. on Radar Meteorology,* Vail, CO, Amer. Meteor. Soc., 31–34.

Linsley, R. K., Jr., M. A. Kohler, and J. L. Paulhus, 1982: *Hydrology for Engineers.* McGraw-Hill, 468 pp.

Mauro, M., 1994: Pictorial Chronology of Tropical Storm Alberto, Part 2. Postprints, *The First WSR-88D Users' Conf.,* Norman, OK, WSR-88D Operational Support Facility and NEXRAD Joint Systems Programming Office, 214–221.

OFCM, 1991: WSR-88D products and algorithms. Federal Meteorological Handbook 11—Part C. FCM-H11C-1991, Washington, DC, 62 pp. [Available from OFCM, 8455 Colesville Road, Suite 1500, Silver Spring, MD 20910.]

Rosenfeld, D., D. B. Wolff, and D. Atlas, 1993: General probability-matched relations between radar reflectivity and rain rate. *J. Appl. Meteor.,* **32,** 50–71.

Seo, D. J., and E. R. Johnson, 1995: The WSR-88D precipitation processing subsystem—An overview and a performance evaluation. *Preprints, Third Int. Symp. on Hydrological Applications of Weather Radars,* Sao Paulo, Brazil, ABRH/IAHR, 222–231.

Wilson, J. W., and E. A. Brandes, 1979: Radar measurement of rainfall—A summary. *Bull. Amer. Meteor. Soc.,* **60,** 1045–1058.